Dyes and Pigments 83 (2009) 391–395

Contents lists available at ScienceDirect

Dyes and Pigments

journal homepage: www.elsevier.com/locate/dyepig

Lipophilic contributions to the solvatochromism of analogous betaines

Marcos Caroli Rezende*, Rubén Oñate, Gabriel Núñez, Moisés Domínguez, Carolina Mascayano

Facultad de Química y Biología, Universidad de Santiago de Chile, Casilla 40, Correo 33, Santiago, Chile

ARTICLE INFO

Article history:
Received 21 April 2009
Received in revised form
11 June 2009
Accepted 12 June 2009
Available online 1 July 2009

Keywords:
Lipophilicity
Solvatochromic phenolate betaines
Dynamics simulation

ABSTRACT

A pair of solvatochromic phenolate betaines that differed only in their lipophilicity was synthesized. Their solvatochromic responses in pure solvents, in a DMSO–MeOH solvent mixture as well as in micellar solutions were different, an observation which confirmed the fact that sensor lipophilicity contributes to the interpretation of solvatochromism. Quantum mechanical calculations reproduced the observed spectral differences. Molecular dynamics simulations shed light on the solute–solvent interactions responsible for their differences in solvent mixtures.

1. Introduction

The spectral behaviour of solvatochromic compounds in solution is associated with their interactions with the solvent. A widely employed approach that identifies and quantifies different solute–solvent contributions to this behaviour is the Kamlet–Taft equation [1,2]. In its simplified form, the transition energy of the solvatochromic band of a solute dye is mainly affected by three factors: the solvent acidity (α), basicity (β) and dipolarity–polarizability (π^*) of the solvent.

$$E_T = c_\alpha\alpha + c_\beta\beta + c_{\pi^*}\pi^* + \text{constant} \quad (1)$$

A linear regression analysis of transition energies in various solvents, for which values of α, β and π^* are available, allows the determination of the corresponding coefficients c_α, c_β and c_{π^*} that may be used as a measure of the relative importance of these factors to the solvatochromism of the investigated compound.

The interpretation of these relative contributions is generally sought in specific interactions between the solvent and the solute. Acidic, or hydrogen-bond-donor (HBD) solvents may affect the solvatochromic charge-transfer band of a dye by partial protonation of its donor and/or acceptor fragment. Basic, or hydrogen-bond-acceptor (HBA) solvents may affect the dye CT band by interacting with acidic sites of the solute. Polarizable solvents will help stabilize dipolar forms of the solute, thus affecting its internal charge-transfer transitions.

An implicit corollary to this approach is that dyes with the same donor and acceptor kernels will respond in the same way to these solvating contributions. In particular, pairs of solvatochromic compounds with different lipophilicity would not show any differences in their solvatochromic behaviour, if they possess the same donor and acceptor fragments.

This corollary has been put to test by El-Seoud et al.,[3] who compared the solvatochromic behaviour of a series of γ-pyridones, which differed in their lipophilicity but had the same phenolate donor and N-alkylpyridinium acceptor fragments. The small spectral differences between the members of this series led the authors to suggest a lipophilic contribution (log P) to the Kamlet and Taft's equation, in the form of expression (2)

$$E_T = c_\alpha\alpha + c_\beta\beta + c_{\pi^*}\pi^* + c_{\log\ P}\log\ P + \text{constant} \quad (2)$$

Their regression analyses, based on this multiparametric equation, led to the conclusion that *all* solvating contributions, expressed by the c_i coefficients, were affected by the variations in the lipophilicity of the dyes.

In the present report we have sought further evidence for unequivocal lipophilic contributions to the spectral behaviour of solvatochromic dyes in solution, besides looking for an interpretation of such contributions.

It is well known that the spectral behaviour of solvatochromic pyridinium phenolate betaines is strongly affected by hydrogen bonds between the solvent and the donor phenolate [4]. We reasoned that, by varying the dye lipophilicity in a region close to this donor fragment, we might be able to obtain an enhanced sensitivity of the betaine to lipophilic contributions of the medium.

* Corresponding author.
E-mail address: marcos.caroli@usach.cl (M.C. Rezende).

0143-7208/$ – see front matter © 2009 Elsevier Ltd. All rights reserved.
doi:10.1016/j.dyepig.2009.06.011

We therefore investigated the solvatochromic behaviour of the pair of vinylogous α-pyridones, **3a**/**b** in pure solvents, in solvent mixtures and in a micro-heterogeneous environment, aqueous micellar solutions of block polymers. In addition, we carried out dynamics simulations of these systems in pure solvents and solvent mixtures, in order to gain a deeper insight into the origins of an eventual lipophilic contribution to their solvatochromic behaviour. This was caused by the observation that, however reasonable the argument that a lipophilic contribution to the Kamlet and Taft equation (2) may appear, one may still argue that, on purely mathematical grounds, the addition of a fourth parameter may improve the fitting of experimental data to any three-parametric model equation. Even when it is demonstrated that the addition of a fourth parameter is statistically significant in a regression equation, the question of the physical meaning of the added parameter remains open. Unlike other solvent contributions like its acidity, basicity or polarizability, which may alter the charge-transfer transition energy of a solvatochromic solute by physically understandable microscopic interactions, the origins of a lipophilic contribution to the solvatochromism of phenolate betaines are less clear. In the present paper we address this question by relating such contributions, as detected by spectroscopic measurements, with a view of the solute–solvent interactions that take place in solutions of these solvatochromic probes, as a result of dynamics simulations.

2. Experimental

2.1. Materials

Melting points were recorded on a capillary Microthermal instrument, and were not corrected. ^{1}H NMR spectra were obtained with a Bruker Avance 400 MHz equipment, employing tetramethylsilane as standard. IR spectra were recorded on a Perkin–Elmer 735B spectrometer. UV–visible spectra were obtained with a diode-array Scinco S-3100 spectrophotometer.

All employed solvents for spectral measurements had an uvasol grade and were purchased from Merck.

The N-methyl-2-(4-hydroxyphenyl)-4,6-diphenylpyridinium fluoroborate **2a** was prepared by reaction of the corresponding 2-(4-hydroxyphenyl)-4,6-diphenylpyrylium fluoroborate **1** [5] with methylamine, as described previously [6]. The corresponding vinylogous α-pyridone **3a** was generated *in situ* by treatment of 5-mL solutions of **2a** with 5–10 μL of 1 M methanolic tetrabutylammonium hydroxide. The resulting coloured solutions had their spectra recorded immediately.

2.1.1. N-octyl-2-(4-hydroxyphenyl)-4,6-diphenylpyridinium fluoroborate (*2b*)

To a stirred solution of 2-(4-hydroxyphenyl)-4,6-diphenylpyrylium fluoroborate **1** [5] (4.1 g, 10 mmol) and n-octylamine (Aldrich) (1.3 g, 10.2 mmol) in dichloromethane (70 mL) was added triethylamine (1.3 g, 12.9 mmol). After stirring the resulting solution for 2 h, acetic acid (0.9 g, 15 mmol) was added and the solution was stirred for 1 h more. The dichloromethane solution was then washed with a dilute solution of fluoroboric acid (10%), then with water, dried over anhydrous sodium sulphate and rotary evaporated. To the residue was then added diethyl ether (50 mL) and the crude, precipitated fluoroborate salt was filtered and crystallized from methanol. The dry pyridinium fluoroborate **2b** weighed 3.0 g (57% yield), m.p. 190–191 °C. Analysis found C, 71.39; H, 6.81; N, 2.81% Calculated for $C_{31}H_{34}NOBF_4$, C, 71.13; H, 6.50; N, 2.68%. IR (KBr) ν_{max} (cm^{-1}) 3400 (OH), 2950, 2870, 1620, 1580, 1510, 1240, 1070 (broad, BF_4^-). ^{1}H NMR ($CDCl_3$) δ 0.82–0.74 (m, 7H, H's from octyl chain), 1.05–0.87 (m, 4H, H's from octyl chain), 1.10–1.20 (m, 2H, $NCH_2CH_2CH_2$), 1.35–1.45 (m, 2H, NCH_2CH_2), 4.45 (t, 2H, J = 7.8 Hz, NCH_2), 7.06 (d, 2H, J = 8.5 Hz, Ar–H *ortho* to OH), 7.57–7.47 (m, 5H, Ar–H), 7.65–7.60 (m, 4H, Ar–H), 7.75–7.70 (m, 2H, Ar–H), 7.78 (d, 2H,J = 6.5 Hz, Ar–H), 7.84 (s, 1H, py-H), 7.88 (s, 1H, py-H).

The corresponding vinylogous N-octyl α-pyridone **3b** was generated *in situ* by treatment of 5-mL solutions of **2b** (2×10^{-4} M) with 5–10 μL of 1 M methanolic tetrabutylammonium hydroxide. The resulting solutions had their spectra recorded immediately.

Confirmation of the structure of the pyridone **3b** was obtained by isolation and characterization of its ^{1}H NMR spectrum of the crude material. To a solution of the pyridinium fluoroborate **2b** (1.0 g, 1.9 mmol) in methanol (10 mL) was added NaOH (80 mg, 2.0 mmol) in methanol (10 mL). The resulting deeply coloured solution was filtered and the filtrate rotary evaporated. The residue was redissolved in acetone, to which drops of methanolic tetrabutylammonium hydroxide had been added, the resulting solution was filtered and the filtrate rotary evaporated. The gummy residue was left standing overnight in a desiccator. The dried betaine, in the form of a purple powder, weighed 0.76 g (92% yield), mp 128–135 °C. ^{1}H NMR ($CDCl_3$) δ 0.82–0.74 (m, 7H, H's from octyl chain), 0.92–1.05 (m, 4H, H's from octyl chain), 1.10–1.20 (m, 2H, $NCH_2CH_2CH_2$), 1.35–1.45 (m, 2H, NCH_2CH_2), 4.52–4.59 (m, 2H, NCH_2), 7.07 (d, 2H, J = 8.6 Hz, Ar–H *ortho* to O^-), 7.38 (d, 2H, J = 8.6 Hz, Ar–H *meta* to O^-), 7.50–7.58 (m, 3H, Ar–H), 7.60–7.72 (m, 6H, Ar–H), 7.75–7.79 (m, 2H, Ar–H, py-H), 7.91 (s, 1H, py-H).

2.2. Theoretical quantum calculations

Structures of vinylogous α-pyridones **3a** and **3b** were optimized with Gaussian98 [7] employing the B3LYP/6-31G* method. The optimized structures were then subjected to single-point calculations employing the semi-empirical ZINDO/S method and configuration interactions involving 1-electron transitions from the 10 highest occupied molecular orbitals to the 10 lowest unoccupied MO's of the molecules.

2.3. Molecular dynamics calculations

Molecular dynamics simulations were carried out in cubic solvent boxes of 40 Å, built for methanol, and for a dimethylsulfoxide–methanol mixture. The structures of the solvents were built and then optimized with Gaussian98 [7] employing the B3LYP/6-31G* method. The number of solvent molecules in each 40-Å box was estimated with an algorithm developed by us, based on the corresponding solvent densities and assuming an ideal behaviour for the solvent mixture [8] The resulting boxes were then built with the Packmol script [9], with 952 molecules in the methanol box. The solvent mixture, assuming equal volumes of each solvent, comprised 476 methanol and 271 DMSO molecules. The solvent molecules were parameterized with the CHARMM33b1 force-field [10].

Structures of the vinylogous pyridones were built with InsightII [11] and optimized with the B3LYP/6-31G* method. Restrained electrostatic potencial (RESP) charges [12] were then obtained with the Gaussian98 package, by single-point calculations on the optimized structures with the HF/6-31G* basis.

The pyridones were inserted into the centre of the box with Packmol [9]. Dynamics simulations of all systems were carried out with NAMD [13], assuming periodic boundary conditions. After heating the systems to 300 K in 3000 steps and equilibrating them in 97 000 steps, simulations were performed with acquisition periods of 2.0 ns. Radial distribution functions (rdf's) of the acquired dynamics were obtained with VMD [14].

3. Results and discussion

3.1. Spectroscopic results

The pair of solvatochromic vinylogous α-pyridones **3** was prepared by basic treatment of the corresponding pyridinium salts **2** by the route below (Scheme 1).

The λ_{max} values of their solvatochromic charge-transfer bands were recorded in various solvents and are listed in Table 1. In spite of their similarities, the different lipophilicities elicited perceptibly different responses to the medium polarity.

This is illustrated in Fig. 1, where the charge-transfer transition energies E_T of compounds **3a** and **3b** in various solvents are plotted against the corresponding $E_T(30)$ polarity values.

The effect of the lipophilicity was further confirmed by a study of preferential solvation of the two compounds in binary mixtures of DMSO/MeOH. The corresponding variations of the transition energies E_T as a function of the DMSO molar fraction in the mixtures are shown in Fig. 2. Again, different responses reflect different patterns of preferential solvation, which may be attributed to their differences in lipophilicity.

The different lipophilicities of the pair of analogs should be especially important in sensing a micro-heterogeneous environment like a micellar system. We therefore compared the λ_{max} values of **3a** and **3b** in aqueous micellar solutions of poloxamers, block polymers of general formula A–B–A where A is a block of hydrophilic polyethyleneoxide (PEO) units and B of a hydrophobic polyisopropyleneoxide (PPO).

Table 2 lists the obtained λ_{max} values for the two analogs in different micellar solutions. In all cases, bathochromic shifts of the solvatochromic band were observed when the betaine lipophilicity was increased. The differences in λ_{max} values of the two analogs were in general larger in micellar solutions than in pure solvents. This may be an indication that in these micro-heterogeneous systems, the intrinsic differences between the responses of **3a** and **3b** increase by the fact that the two probes sense different microenvironments. The more lipophilic analog **3b** should be inserted more deeply into the hydrophobic core of the micelle than **3a**, leading to significant bathochromic shifts of its λ_{max} values, when compared with compound **3a**.

3.2. Dynamics simulation results

The above results support the contention that the lipophilicity of a phenolate betaine affects its solvatochromic behaviour. In order to understand how this factor affects its CT transition energy, we carried out dynamics simulations of the investigated systems, in methanol and in a DMSO–MeOH solvent mixture.

A picture of the solvation shell around a given atom may be obtained from radial distributions of the solvent molecules as a function of the distance between the atom and the solvent molecules. In our analyses we chose the phenolate oxygen as the solute atom, because of the well-known sensitivity of this donor moiety to the solvatochromic response of phenolate betaines to the hydrogen-bonding solvent. Radial distributions based on the solute–solvent O–O distance were then obtained in pure methanol and in a DMSO-methanol mixture for the two pairs of betaines.

Radial distribution functions (rdf's) for the betaine pair in methanol were rather similar. The small but perceptible differences between compounds **3a** and **3b** in this solvent could not be reproduced by an approach based purely on classical mechanics, that ignored quantum mechanical effects. However, these differences emerged very clearly when we estimated the $S_0 \rightarrow S_1$ transition energies of dyes **3a** and **3b** by means of a semi-empirical calculation. After optimizing both molecules with a hybrid DFT method (B3LYP//6-31G*), we carried out single-point calculations with the ZINDO/S method, employing configuration interactions involving 1-electron transitions from the 10 highest occupied molecular orbitals to the 10 lowest unoccupied MO's of the molecules.

The resulting first singlet was essentially a HOMO–LUMO transition for both compounds, with calculated λ_{max} values of 502 nm ($f = 1.072$) and 510 nm ($f = 0.997$) for the N-methyl **3a** and the N-octyl derivative **3b**, respectively. These gas-phase values were reasonably close to the experimental absorption values of these compounds in solvents of medium or low polarity, like DMF and chloroform (Table 1). More important, the estimated bathochromic shift of 10 nm, when the more lipophilic vinylogous pyridone **3b** was compared with **3a**, was in the range of experimental shifts in less polar media, listed in Table 1. The observation of such shifts in non polar media, reproduced by gas-phase calculations, rules out dye aggregation in solution as a possible cause for the different behaviour of analogs **3a**/**3b**. Aggregation might lead to a different spectral response of compound **3b** in polar solvents, but not in non polar media. In addition, the effect should be completely absent in a single-molecule, gas-phase calculation. The different λ_{max} values of dyes **3a** and **3b**, predicted theoretically by the CI calculations, suggest that the size of the N-alkyl substituent affects the electronic

Table 1
Values of λ_{max} of the solvatochromic band of compounds **3a** and **3b** in various solvents.

Solvent	λ_{max}/nm	
	3a	**3b**
Water	389	394
Methanol	432	435
Ethanol	454	456
1-Butanol	472	474
2-Propanol	486	489
DMSO	531	537
DMF	556	567
Chloroform	538	545

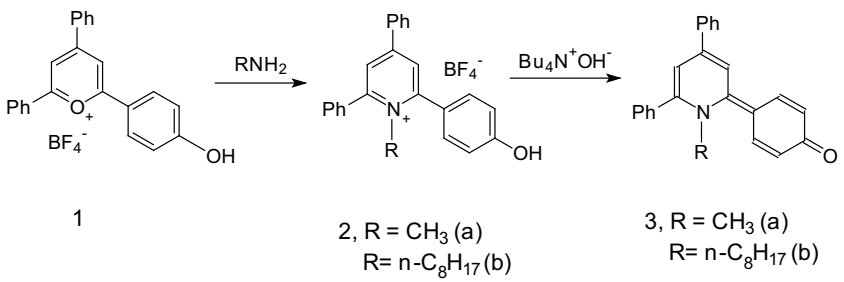

Scheme 1. Preparation of vinylogous pyridones **3**.

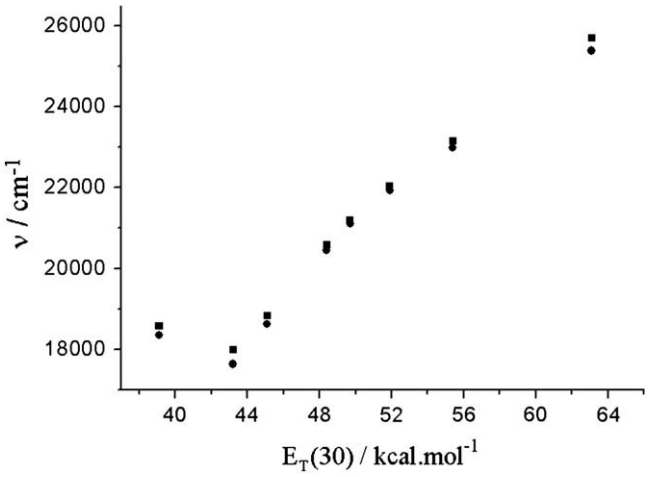

Fig. 1. Variations of the transition energies, expressed in wavenumber values ν, of betaines **3a** (■) and **3b** (●) with the $E_T(30)$ polarity value of the solvent.

excitations of these betaines. This may be the result of slightly different optimized geometries of compounds **3a** and **3b**, employed in the single-point ZINDO/S calculations. In fact, although the 4-oxyphenyl substituent has a similar degree of coplanarity with the pyridinium ring in both compounds (dihedral angle of 30° in **3a** and 35° in **3b**), the 6-phenyl substituent is much less coplanar in **3a** (dihedral angle of −53°), attaining a nearly perpendicular configuration in **3b** (dihedral angle of −102°). Such geometrical differences lead to slightly different HOMO and LUMO densities for both compounds – the 6-phenyl substituent has little participation in the LUMO of **3a** and practically none in the LUMO of **3b** – leading to different $S_0 \rightarrow S_1$ transition energies.

Dynamics simulations proved more useful in the interpretation of the different spectral responses of compounds **3a** and **3b** in a solvent mixture. In the 1:1 v/v (*ca.* 2:3 molar ratio) DMSO–MeOH mixture, the cybotactic region around the phenolate oxygen of betaines **3a** and **3b** differed appreciably, as can be deduced from an inspection of the rdf's of Figs. 3 and 4. For the N–Me derivative **3a**, an average of 3.8 methanol molecules comprised the first solvation shell, at 2.7 Å distance from the oxygen atom. For the N-octyl analog **3b**, the solvation shell comprised only 2 methanol molecules, at a peak distance of 2.8 Å (see Fig. 3). Thus, the more lipophilic

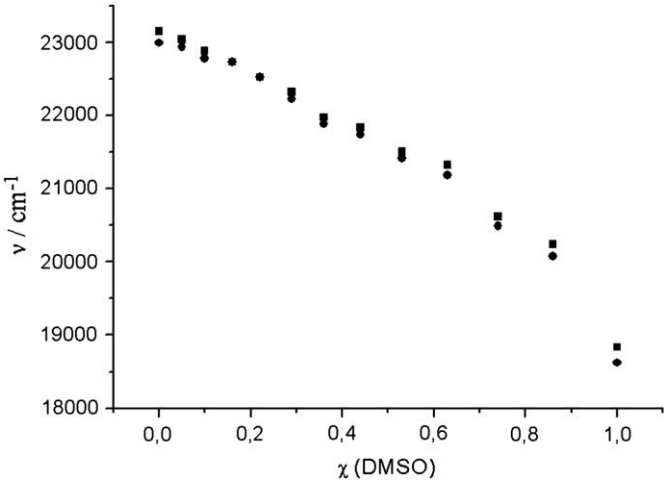

Fig. 2. Variations of the transition energies E_T, in wavenumber values, of betaines **3a** (■) and **3b** (●) in MeOH–DMSO solvent mixtures, with the DMSO molar fraction χ.

Table 2
Variation of the λ_{max} value of the solvatochromic band of betaines **3a** and **3b** in aqueous basic (0.1 M NaOH) solutions of poloxamer micelles.

Poloxamer[a]	% in weight of PEO	Molecular weight	λ_{max}/nm	
			3a	**3b**
–[b]	–	–	389	394
P-407[c]	70	12 000	402	424
P-237[c]	70	7700	391	418
P-401[c]	10	4400	393	403
P-105[c]	50	1900	391	403

[a] Poloxamers are characterized by their molecular weight and weight percentage of the polyethyleneoxide (PEO) block.
[b] In an aqueous NaOH 0.1 M solution, in the absence of any micelle.
[c] Poloxamer concentration equal to 1×10^{-3} M, betaine concentrations equal to 1.9×10^{-4} M.

derivative of the pair is solvated by a smaller number of hydrogen-bonding methanol molecules, situated farther away from the phenolate oxygen. As a result, this compound experiences a less "polar" environment, in line with the bathochromic shift observed for its CT band when compared with analog **3a** (Fig. 3).

The differences in solvation of the two phenolate betaines were even more apparent when the DMSO co-solvent was considered (Fig. 4). The rdf of compound **3a** exhibited a broad DMSO solvation shell, centered around 7.0 Å from the phenolate oxygen, and

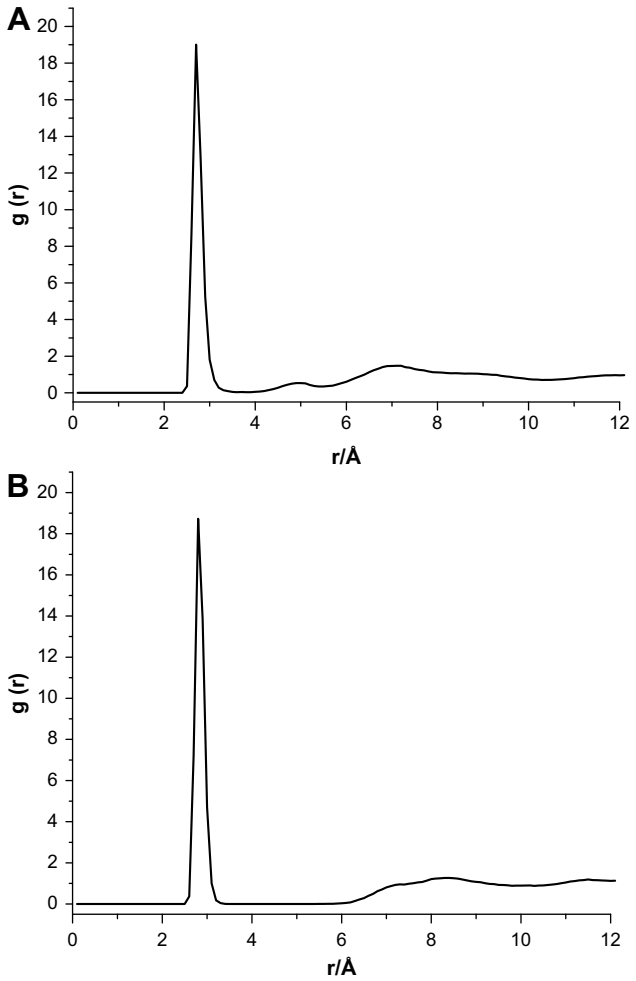

Fig. 3. Radial distribution of methanol molecules around the phenolate oxygen of betaines **3a** (A) and **3b** (B) in a 1:1 v/v MeOH–DMSO mixture, derived from the solute–solvent O–O distances.

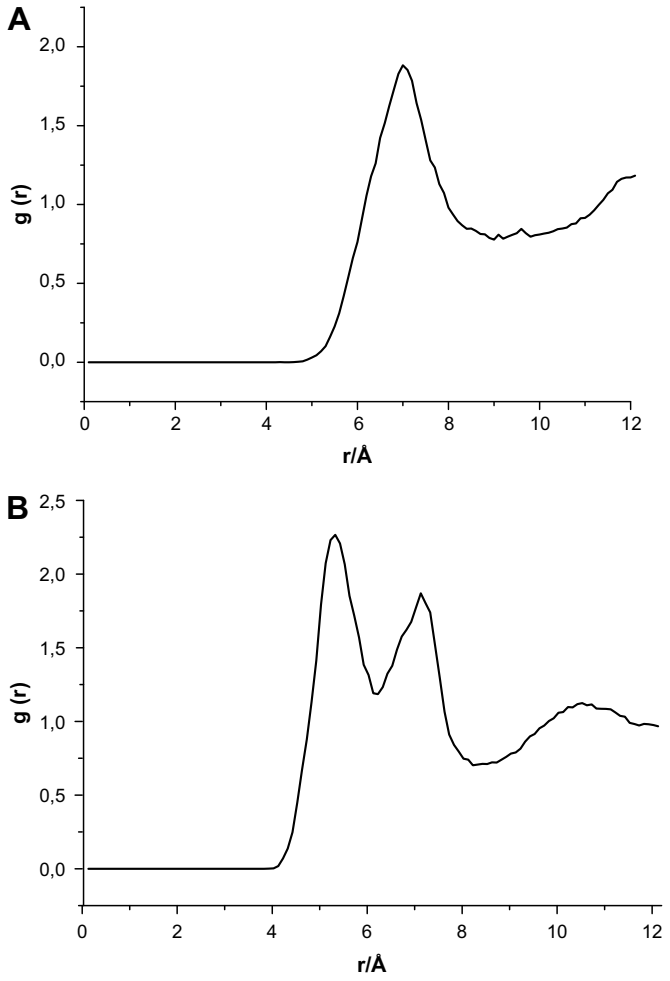

Fig. 4. Radial distribution of DMSO molecules around the phenolate oxygen of betaines **3a** (A) and **3b** (B) in a 1:1 v/v MeOH–DMSO mixture, derived from the solute–solvent O–O distances.

containing an average of 9.6 solvent molecules. By contrast, the rdf of compound **3b** exhibited a very different pattern, with two broad DMSO shells, at 5.3 and 7.1 Å from the solute oxygen atom, and a total of 12.6 solvent molecules. These results complement the observations made above for the betaine interactions with the methanol co-solvent. Here the more lipophilic betaine **3b** has a solvation shell closer to its phenolate oxygen and richer in the aprotic, less "polar" co-solvent DMSO than its analog **3a**.

In conclusion, we have shown that lipophilicity is a factor to be considered in the interpretation of the solvatochromic response of phenolate betaines in pure solvents, in solvent mixtures and in micellar solutions, thus confirming and widening recent observations made by other authors [3]. In the past, when using a more lipophilic analog of a solvatochromic probe to sense non polar environments [15–17], one had tacitly assumed that the solvatochromic response of the two probes was not affected by their different lipophilicities. The present paper corroborated previous observations that this is not true. Different responses obtained in micellar systems from pairs of analogous probes of different lipophilicities have also been taken as evidence of different microenvironments sensed by the probes [18–21]. According to our results, such interpretations should be made with caution, because analogous probes of different lipophilicities present intrinsically different responses even in homogeneous media.

We have also shown in the present paper that the lipophilic contribution, incorporated in the multiparametric Kamlet–Taft equation, finds its interpretation in theoretical calculations. The different spectral responses of analogs **3a** and **3b** in pure solvents could be reproduced by quantum chemical calculations employing configuration interactions and the ZINDO/S method on structures previously optimized by a DFT option. Their different responses in solvent mixtures could be attributed by dynamics simulations to different preferential solvations of their donor moieties. The donor phenolate moiety of the more hydrophilic compound **3a** was more solvated by methanol than that of analog **3b**. As a result, a hypsochromic shift of the solvatochromic λ_{max} value of **3a** relative to that of **3b** would be expected, in line with what was observed experimentally. Thus, our results provide a physical picture, based on microscopic interactions in solution, to account for the effect of lipophilicity on the solvatochromism of analogous betaines.

Acknowledgments

This work was financed by Fondecyt project 1070124. We are grateful to the computational time provided by Project DICYT/USACH "Apoyo Complementario."

References

[1] Kamlet MJ, Abboud JL, Taft RW. J Am Chem Soc 1977;99:6027.
[2] Kamlet MJ, Abboud JL, Abraham MH, Taft RW. J Org Chem 1983;48:2877.
[3] Martins CT, Lima MS, El Seoud OA. J Org Chem 2006;71:9068–79.
[4] Reichardt C. Solvents and solvent effects in organic chemistry. 3rd ed. Weinheim: Wiley–VCH; 2003.
[5] Aliaga C, Galdames JS, Rezende MC. J Chem Soc Perkin Trans2 1997:1055–8.
[6] (a) Galdames JS, Rezende MC. J Chem Res Synop 1998:106–7.
(b) Galdames JS, Rezende MC. J Chem Res Miniprint 1998:601–13.
[7] Frisch MJ, Trucks GW, Schlegel HB, Scuseria GE, Robb MA, Cheeseman JR, et al. Gaussian 98. Pittsburgh PA: Gaussian, Inc; 1998.
[8] Oñate R, Domínguez M, Núñez G. MOLECv1.0, http://code.google.com/p/molecv1/; 2008.
[9] Martínez JM, Martínez LJ. Comput Chem 2003;24:819–25.
[10] Brooks BR, Bruccoleri RE, Olafson BD, States DJ, Swaminathan S, Karplus M. J Comput Chem 1983;4:187–217.
[11] InsightII user guide. San Diego: Accelrys; 1998.
[12] Bayly CI, Cieplak P, Cornell WD, Kollman PA. J Phys Chem 1993;97:10269–80.
[13] Phillips JC, Braun R, Wang W, Gumbart J, Tajkhorshid E, Villa E, et al. Comput Chem 2005;26:1781–802.
[14] Humphrey W, Dalke A, Schulten K. J Mol Graphics 1966;14:33–8.
[15] Reichardt C, Schäfer G. Liebigs Ann 1995:1579–82.
[16] Reichardt C, Löbbecke S, Mehrampour MA, Schäfer G. Can J Chem 1998;76:686–94.
[17] Gillson S, Rappon M. J Mol Liquids 2006;128:108–14.
[18] Hof M, Lianos P, Laschewsky A. Langumuir 1997;13:2181–3.
[19] Ali Awan M, Shah SS. Colloids Surfaces A 1997;122:97–101.
[20] Mchedlov-Petrossyan NO, Vodolazkaya NA, Reichardt C. Colloids Surfaces A 2002;205:215–29.
[21] Moyano F, Silber JJ, Correa NM. J Coll Int Sci 2008;317:332–45.